

Experimental Study of a Novel Adaptive Controller for Active Vibration Isolation

Lei Zuo, Jean-Jacques E. Slotine, and Samir A. Nayfeh

Abstract— Adaptive control has drawn attention for active vibration isolation and vehicle suspensions because of its potential to perform in the presence of nonlinearities and unknown or time-varying parameters. Model-reference adaptive control has been used to force the plant to track the states or certain outputs of the ideal reference model. In this paper, we study application of a new adaptive approach, “model-reaching” adaptive control, to achieve the ideal multi-DOF isolation effect of a skyhook target without using a model reference. We define a dynamic manifold in terms of the states of the plant, rather than the error of the plant tracking of the reference. Then we derive an adaptive control law based on Lyapunov analysis to make the isolation system reach the dynamic manifold while estimating the unknown parameters. Compared with the conventional model-reference adaptive algorithm for vibration isolation, the proposed adaptive control eliminates the need for measurement of base vibration and has the potential to guarantee the transient performance. The effects of geophone dynamics are also discussed. We carry out an experimental investigation based on a realistic plant with friction, demonstrate the effectiveness of the proposed adaptive control, and show that the target dynamics of the skyhook isolator are attained. The convergence of the parameter adaptation in the experiment is also examined.

Index Terms— Vibration isolation, Vehicle suspension, Adaptive control, Sliding control, Model reaching, Skyhook damping

I. INTRODUCTION

Active vibration isolation systems or suspensions have become necessary in many applications to compensate for the low-frequency inadequacy of passive vibration isolation. A variety of control techniques, such as PID or lead-lag compensation, LQG/H₂, H_∞, μ -synthesis, and feedforward control, have been used in active systems (e.g., [1], [2], [3], [4], [5], [6], [7], [8], [9]).

One of the classical concepts in the literature on vibration isolation is the “skyhook” damper proposed by Karnopp in 1974 [10], [1]. The skyhook damper is a virtual configuration where the damper is connected with a virtual inertial “sky.” Figure 1(a) shows a SDOF skyhook isolator. In passive systems, the damper can be connected only to the base since there is no practical inertial sky, as shown in Figure 1(b). The vibration transmissions of the two configurations are compared in Figure 2. From which we see that whereas there exists a tradeoff between high- and low-frequency performances in (b), there is no such conflict in the skyhook system. The skyhook configuration also eliminates the tradeoff between rejection of disturbances

directly acting at the payload and isolation from ground vibration.

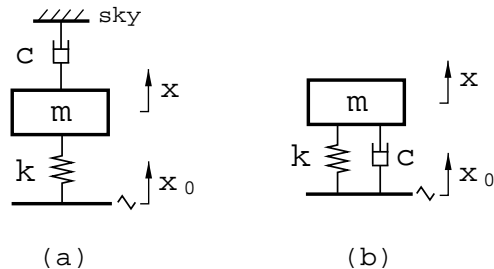


Fig. 1. (a) Skyhook configuration, (b) the classical configuration

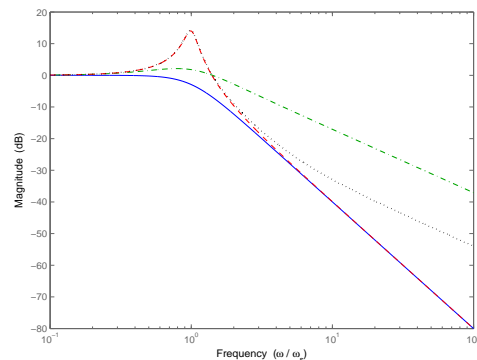


Fig. 2. Vibration transmission from ground to platform of the two configurations ($c = 2\zeta\omega$, $k = \omega^2$). Skyhook with $\zeta = 0.7$ (solid), skyhook with $\zeta = 0.1$ (dash), classical with $\zeta = 0.7$ (dash-dot), classical with $\zeta = 0.1$ (dot).

Because of these advantages, the skyhook configuration has been a target in many isolation or suspension systems. Sliding control has been used to attain the desired skyhook effect in the presence of uncertainties [11], [12], [13]. Adaptive control has attracted a great deal of attention because it does not require prior knowledge of the plant parameters and works well in systems with nonlinearities and time-varying of parameters. Sunwoo et al [14] used model-reference adaptive control for vehicle suspensions by tracking the states of the desired skyhook model. Alleyne and Hedrick [15] considered the nonlinear dynamics of an electro-hydraulic actuator and developed an adaptive control for tracking the ideal skyhook force of a suspension. Wang and Sinha [16] proposed a model-reference adaptive algorithm to achieve multi-DOF skyhook isolation by tracking all of the states. Bakhtiari-Nejad and Karami-Mohammadi [17] considered the flexible mode of a vehicle body and

The authors are with the Department of Mechanical Engineering, Massachusetts Institute of Technology, Cambridge, MA 02139 (Email: leizuo@mit.edu, jjs@mit.edu, nayfeh@mit.edu)

used adaptive control to track the states of a reference model of an LQ-controlled skyhook system. Zhang and Alleyne [18] proposed a position-tracking schedule with adaptive control to overcome the limitations of an electro-hydraulic actuator on force tracking.

These previous studies share a common point: they use an adaptive algorithm to track (or follow) the states or certain outputs of the desired isolation model. This model-reference adaptive control generally requires measurement of ground disturbance (velocity or acceleration) as an input to the reference model, increasing the cost and complexity of such systems, and even making the implementation impractical in some cases. For example, it is difficult to sense the road surface while a vehicle is moving. (In the literature, a sensor is usually mounted at the wheel hub, but the measurement is valid only below approximately 10 Hz.)

In this paper we experimentally study a novel adaptive control scheme for vibration isolation without employing model-reference tracking [13]. The idea is to design a dynamic manifold in terms of the states of the plant which corresponds to the isolation target then to use adaptive control to drive the system onto this manifold while updating the system parameters. This adaptive algorithm eliminates the foregoing shortcoming of reference-tracking based adaptive control, and it also has advantages for transient performance. The effect of geophone dynamics on the stability is also examined. We carry out an experimental study based on a realistic plant with friction and demonstrate the effectiveness of the proposed adaptive control for vibration isolation. The convergence of parameter estimates is also discussed.

II. ADAPTIVE CONTROL FOR VIBRATION ISOLATION WITHOUT MODEL REFERENCE

A. Isolation Plant and Target Dynamics

Suppose an n -degree-of-freedom isolated platform is subject to excitation from vibration of the ground or base. The governing equation takes the form:

$$M\ddot{x} + C(\dot{x} - \dot{x}_0) + K(x - x_0) + F_{rc} = Bu \quad (1)$$

where M , C , and K are mass, damping, and stiffness matrices of dimension $n \times n$; F_{rc} is the friction force matrix; B is a $r \times n$ ($r \geq n$) matrix determined from actuator placement with full-row rank; x is the vector of displacements; x_0 is the vector of ground disturbances; and u is the control force vector. Although many elaborate friction models to account for static, dynamic, and Stribeck frictions are available, in the present study we take the force F_{rc} to obey the Coulomb friction model

$$F_{rc} = F \text{sgn}(\dot{x} - \dot{x}_0)$$

where sgn denotes the signum function. The parameters of the M , C , K , and F matrices are generally unknown. The matrix B is determined by the geometric location of the actuators and sensors, which is relatively easy to obtain.

The ideal ‘‘skyhook’’ system is selected as the target. The target dynamics of an n -th order skyhook isolator take the form

$$\bar{M}\ddot{x} + \bar{C}\dot{x} + \bar{K}(x - x_0) = 0$$

Because the mass matrix \bar{M} is positive definite, we can simplify the skyhook target to the form

$$\dot{x} + \bar{C}\dot{x} + \bar{K}(x - x_0) = 0 \quad (2)$$

where usually \bar{C} and \bar{K} are block-diagonal matrices, which suggests that we achieve the skyhook isolation for each of the variables x_i , $i = 1, 2, \dots, n$.

B. Model-Reaching Adaptive Control of Isolation

As mentioned in the introduction, the conventional way to achieve the skyhook effect using an adaptive algorithm is to control the plant to follow the states or output of the target and use the tracking errors for parameter adaptation. In this section, we describe a new adaptive control algorithm, which we call model-reaching adaptive control [13].

Define a dynamic manifold in the state space

$$\sigma = \dot{x} + (sI + \bar{C})^{-1}\bar{K}(x - x_0) \quad (3)$$

where s is the Laplace operator. Then on the manifold $\sigma = 0$, we have

$$\dot{x} + (sI + \bar{C})^{-1}\bar{K}(x - x_0) = 0 \quad (4)$$

which is exactly the target skyhook isolation

$$\dot{x} + \bar{C}\dot{x} + \bar{K}(x - x_0) = 0$$

In the following, we will describe a method by which adaptive feedback control can drive the dynamics of the plant to reach the manifold $\sigma = 0$ when the parameters of K , C , and M are not known.

Let us first rearrange the unknown parameters in the matrices M , C , and K into a column vector a and denote

$$K(x - x_0) + C(\dot{x} - \dot{x}_0) - M(sI + \bar{C})^{-1}\bar{K}s(x - x_0) + F \text{sgn}(\dot{x} - \dot{x}_0) := Y a \quad (5)$$

where Y is a matrix with proper dimension composed of \dot{x} , $x - x_0$, and $\dot{x} - \dot{x}_0$, which can be measured. (In practice, the relative velocity $\dot{x} - \dot{x}_0$ can also be estimated from $x - x_0$.) Note that in (5) the unknown matrices K , C , M , and F show up linearly.

Next, using Lyapunov analysis and Barbalat’s lemma, we derive the control and adaptation laws using a procedure similar to that in [19]. We choose a positive-definite Lyapunov function as

$$V(\sigma, \tilde{a}) = \frac{1}{2}\sigma(t)^T M \sigma(t) + \frac{1}{2}\tilde{a}(t)^T P^{-1}\tilde{a}(t) \quad (6)$$

where the vector $\sigma(t)$ is defined by (3), M is the (positive definite) mass matrix of the system, P is a pre-selected (constant) symmetric positive definite matrix, and the vector of $\tilde{a}(t)$ is the error vector of on-line estimates of the parameters a . The time derivative of $V(\sigma, \tilde{a})$ is

$$\dot{V}(\sigma, \tilde{a}) = \sigma(t)^T M \dot{\sigma}(t) + \dot{\tilde{a}}(t)^T P^{-1}\tilde{a}(t) \quad (7)$$

Using (1) and (3), we obtain

$$\begin{aligned}\dot{V}(\sigma, \tilde{a}) &= \sigma(t)^T [M\ddot{x} + M(sI + \bar{C})^{-1} \bar{K}(\dot{x} - \dot{x}_0)] + \dot{\tilde{a}}(t)^T P^{-1} \tilde{a}(t) \\ &= \sigma(t)^T [Bu - K(x - x_0) - C(\dot{x} - \dot{x}_0) - F \text{sgn}(\dot{x} - \dot{x}_0) \\ &\quad + M(sI + \bar{C})^{-1} \bar{K}s(x - x_0)] + \dot{\tilde{a}}(t)^T P^{-1} \tilde{a}(t)\end{aligned}\quad (8)$$

Substituting the expression (5) into the above equation, we obtain

$$\dot{V}(\sigma, \tilde{a}) = \sigma(t)^T (Bu - Ya) + \dot{\tilde{a}}(t)^T P^{-1} \tilde{a}(t)\quad (9)$$

We choose the control-force vector as

$$u = B^{-1} [Y\hat{a}(t) - k_d \sigma(t)]\quad (10)$$

where the matrix k_d is a selected positive definite matrix of $n \times n$, the vector \hat{a} is the on-line estimate of the unknown parameters of a , and the estimation error $\tilde{a} = \hat{a} - a$. Then we substitute (10) into (9) and obtain

$$\begin{aligned}\dot{V}(\sigma, \tilde{a}) &= -\sigma^T k_d \sigma + \sigma^T Y(\hat{a} - a) + \dot{\tilde{a}}^T P^{-1} \tilde{a} \\ &= -\sigma^T k_d \sigma + (\sigma^T Y + \dot{\tilde{a}}^T P^{-1}) \tilde{a}\end{aligned}\quad (11)$$

Hence, if we choose the parameter adaptation law as

$$\dot{\hat{a}}(t) = \dot{\tilde{a}} = -PY^T \sigma(t)\quad (12)$$

we have

$$\dot{V}(\sigma, \tilde{a}) = -\sigma(t)^T k_d \sigma(t)\quad (13)$$

Then $\dot{V}(\sigma, \tilde{a})$ is negative semi-definite. We can further prove that $\ddot{V}(\sigma, \tilde{a})$ is bounded. Thus, according to the Lyapunov theorems and Barbalat's lemma [20], we conclude that $\sigma(t) \rightarrow 0$ as $t \rightarrow \infty$. Therefore, using the adaptive control (10) and (12), we drive the states of the system to reach the manifold (3) upon which the plant achieves the target dynamics of shyhook isolation (2). We call this adaptive algorithm model-reaching adaptive control. Note that we do not need a measurement of base vibration.

Furthermore, the manifold (3) is dynamic, in the sense that there is a Laplace operator therein. So theoretically we can choose its initial state such that $\sigma(t=0) = 0$ and transient performance is guaranteed.

The adaptive control works even if payload mass or other parameters change (slowly). The selection of the constant matrices of P and k_d can be used to adjust the time of adaptation and the time to reach the manifold. Like model-reference adaptive control, the adaptation law (12) cannot ensure that the parameters converge to their true values unless the system is persistently excited (e.g., [20]); that is, there exist α and δ such that

$$\int_{t_0}^{t_0+\delta} Y^T Y dt \geq \alpha I, \quad \forall t_0 \geq 0\quad (14)$$

C. Effect of Geophone Dynamics

In the foregoing derivation of the adaptive controller, we assume that the absolute velocity of the isolated platform can be measured. But in practice, velocity measurements are only valid above a certain frequency. For a geophone

sensor the measured output \hat{x}_i and the actual velocity \dot{x}_i generally take the form

$$\hat{x} = \frac{s^2}{s^2 + 2\zeta_g \omega_g s + \omega_g^2} \dot{x}\quad (15)$$

where ω_g and ζ_g are the resonance frequency and damping ratio of the geophone sensor. With the measurement \hat{x} , the actual dynamic manifold becomes

$$\hat{\sigma} = \hat{x} + (s + \bar{C})^{-1} \bar{K}(x - x_0)\quad (16)$$

Suppose that the target dynamics for all the degrees of freedom are selected as skyhooks with frequency ω_s and damping ζ_s ; that is, $\bar{K} = \text{diag}([\omega_s^2, \omega_s^2, \dots, w\omega_s^2])$ and $\bar{C} = \text{diag}([2\zeta_s \omega_s, 2\zeta_s \omega_s, \dots, 2\zeta_s \omega_s])$. Using the Routh-Hurwitz criterion, we conclude that the dynamics of x on the actual dynamic manifold $\hat{\sigma} = 0$ are stable if

$$\frac{\omega_s}{\omega_g} > \frac{\zeta_s}{\zeta_g} + \frac{\zeta_g}{\zeta_s}\quad (17)$$

This suggests that the geophone resonance frequency should be smaller than half of the resonance frequency of the target skyhook isolator.

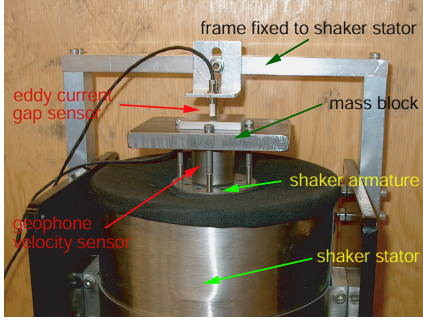
III. EXPERIMENT AND RESULTS

In order to verify the control strategy and to demonstrate the effectiveness of the proposed adaptive control, we carry out an experimental investigation. An electromagnetic shaker is adapted so that the armature (mounted via flexures to the stator) and a mass block fixed on it compose a SDOF isolated platform and the voice coil serves as actuator. A magnetically-shielded geophone is mounted onto the platform to measure its absolute velocity \dot{x}_0 , and an eddy-current gap sensor is used to measure the relative displacement $x - x_0$, as seen in Figure 3(a). The shaker is set on a wood benchtop. Because the mass of the platform is far less than that of the base (stator and bench), we can ignore the effect of the control force u on base vibration. A second geophone is set on the base to monitor its vibration, but is not used in control. The sensor signals are connected to 16-bit analog-to-digital converters (ADC) after gain adjustment. Low-pass filters (at 3 kHz) are used to reduce high-frequency noise and aliasing. A 14-bit digital-to-analog converter (DAC) and a voltage-to-current power amplifier are used for actuation. The control is implemented using a dSpace 1103 board hosted by a PC. We set the sampling frequency to 10 kHz. The whole system is shown in Figure 3.

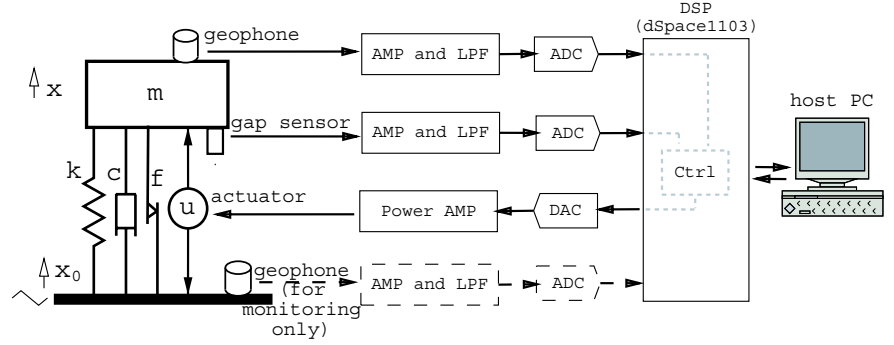
This is a single-DOF isolation platform. If we take the control signal u as voltage, B is a scalar with units of N/volt. We normalize B to one and write the plant model as

$$m\ddot{x} + c(\dot{x} - \dot{x}_0) + k(x - x_0) + f \text{sgn}(\dot{x} - \dot{x}_0) = u$$

where k , c , m , and f are unknown. Note that due to the normalization of B , the units of k , c , m and f are now N/m/(N/volt), N·s/m/(N/volt), kg/(N/volt) and N/(N/volt),



(a)



(b)

respectively. According to the parameterization (5) in Section 2, we write

$$a = [k, c, m, f]^T \quad (18)$$

$$Y = \left[x - x_0, \dot{x} - \dot{x}_0, -\frac{\bar{k}s}{s + \bar{c}}(x - x_0), \text{sgn}(\dot{x} - \dot{x}_0) \right] \quad (19)$$

where $\dot{x} - \dot{x}_0$ is estimated by passing $x - x_0$ through a filter $s/(1 + \tau s)$ with a pole at 1.5 kHz. The passive isolation system (open-loop) has a natural frequency of around 12 Hz, and we set our target as a skyhook isolator with a natural frequency of 1.2 Hz and damping ratio of 0.7. To satisfy the condition (17) we correct our geophone corner frequency from 5 Hz to 0.5 Hz and damping to 0.7 using a second-order circuit. In the following results we select the constant k_d as 3000 and the constant matrix P as $\text{diag}([1e14, 1e10, 3e8, 1e3])$.

We employ a second shaker as a reaction-mass actuator to excite the base. Figure 4 shows the time responses when the adaptive control is turned on while the base is excited at 10 Hz by the second shaker in addition to ambient excitation. The initial guesses of the parameters k , c , m , and f are selected as zeros. In this figure, we show the measured velocity \dot{x} of the platform, measured velocity \dot{x}_0 of base vibration, and the calculated velocity \dot{x}_s of target skyhook isolator. We see that the vibration of the passive isolated platform (control off) is amplified, since the base vibration is close to the resonant frequency of 12 Hz. After the control turns on, the platform isolation tends to the target skyhook output in a few seconds. Figure 6 shows the zoomed time response of the controlled isolator. We see that the proposed adaptive algorithm can effectively control the platform to match the target skyhook isolation.

In the zoomed velocity plots there are pulses when the velocity crosses zero; this is because the Coulomb friction model is not valid at zero velocity. The other small residual errors are due to sensor noise and some unmodelled dynamics (such as the 3 kHz low-pass filters for the sensors). For comparison, we also implement the model-reaching adaptive control by ignoring the friction term in the model. Figure 5 shows the zoomed time response of such a controlled isolator with the same P and k_d . Comparing Figure 6 and 5, we see that although the Coulomb friction model is not valid at zero velocity, we obtain a performance

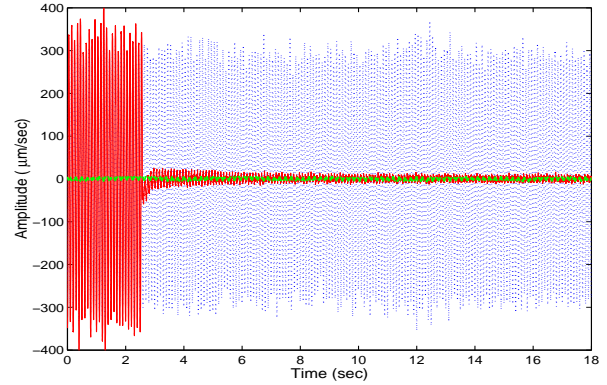


Fig. 4. Time response of isolation system when adaptive control turns on under 10 Hz base excitation. Base velocity (dot), platform velocity (solid), target skyhook velocity (dash)

improvement by taking it into account. The effect of the friction compensation can also be seen in the control effort (in voltage) shown in Figure 7.

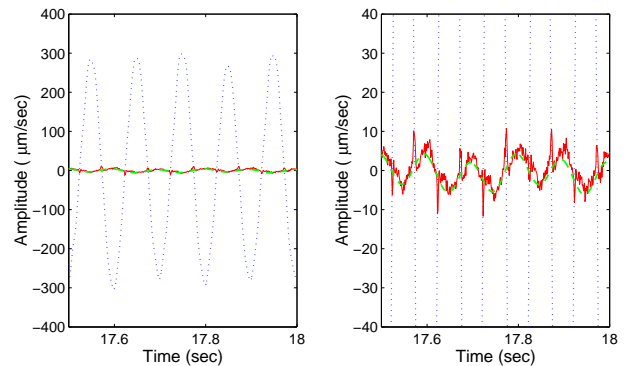


Fig. 5. Zoomed time response of isolation system with adaptive control under 10 Hz base excitation. Base velocity (dot), platform velocity (solid), target skyhook velocity (dash)

The parameter convergence for 10 Hz base excitation is shown in Figure 8. The stiffness, damping, and friction converge to reasonable values close to their off-line estimates. But the estimated mass is negative. This can be explained by using the condition (14) to check for persistent excitation by starting at any time $t_0 \geq 0$ and checking the integral

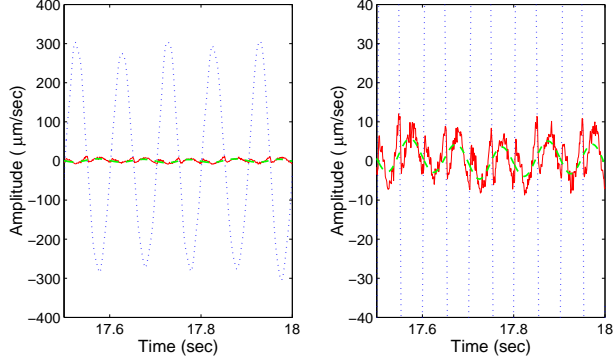


Fig. 6. Zoomed time response of isolation system with adaptive control without accounting friction in the model under 10 Hz base excitation. Base velocity (dot), platform velocity (solid), target skyhook velocity (dash)

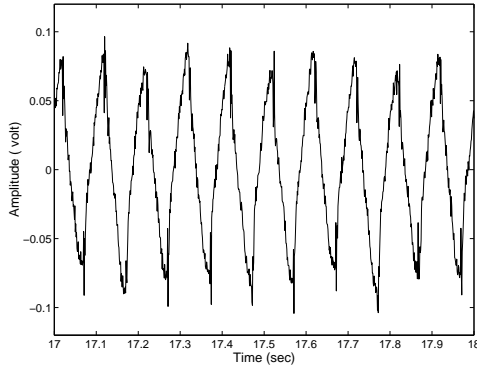


Fig. 7. Control effort in voltage under 10 Hz base excitation

over any time interval δ . One typical value of the integral $\int_{t_0}^{t_0+\delta} Y^T Y dt$ over 2 seconds for 10 Hz base excitation is

$$\begin{bmatrix} 2.638e-11 & 3.512e-11 & -1.455e-9 & 2.483e-8 \\ 3.512e-11 & 3.783e-7 & -3.095e-8 & 7.759e-4 \\ -1.455e-9 & -3.095e-8 & 8.275e-8 & -6.156e-5 \\ 2.483e-8 & 7.759e-4 & -6.156e-5 & 2.0000 \end{bmatrix}$$

whose singular values are 2.0, 8.64e-8, 7.18e-8, and 0. The integrals of other time intervals are similar. This indicates that the system is not persistently excited. Examining the expression for Y given by (19), we can understand this result more intuitively. With our choice of skyhook target with a corner frequency of 1.2 Hz and a damping ratio of 0.7, $\frac{k_s}{s+\bar{c}}$ is a high pass filter at 1.68 Hz. Thus for 10 Hz excitation, the third element $-\frac{k_s}{s+\bar{c}}(x-x_0)$ of Y closely approximates $-\bar{k}(x-x_0)$, which is proportional to the first element $x-x_0$ of Y . Hence the mass adaptation error can be approximately cancelled by a contribution from the stiffness, and therefore their adaptation needn't converge the actual values. However, the parameter convergence is not important so long as we achieve the desired skyhook isolation.

Figure 9 shows the time responses of the isolated platform when the adaptive control is turned on while the base is subject to random excitation by the shaker plus the ambient disturbance. (The actual spectrum of the base

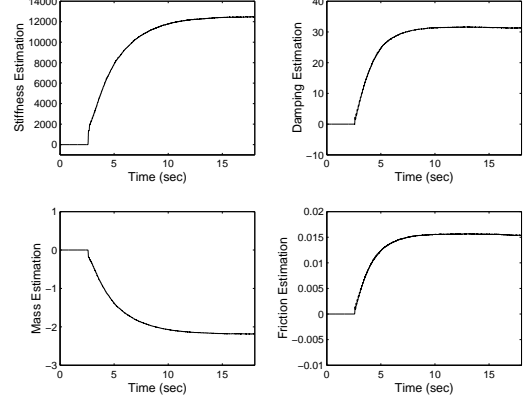


Fig. 8. Convergence of parameter estimations under 10Hz base excitation: stiffness \hat{k} , damping \hat{c} , mass \hat{m} , and friction \hat{f}

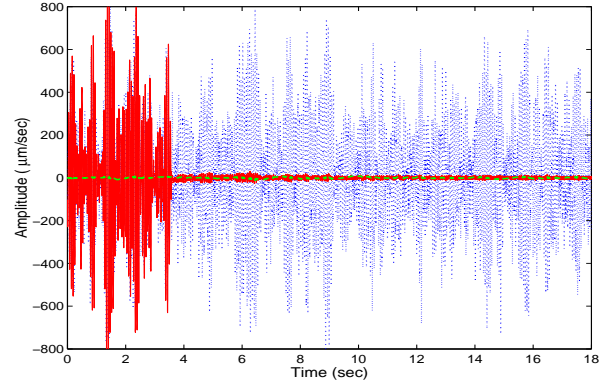


Fig. 9. Time response of isolated platform when adaptive control turns on under random excitation. Base velocity (dot), platform velocity (solid), target skyhook velocity (dash)

vibration is not white, because of the bench dynamics and the bandwidth limitation of reaction-mass excitation by the second shaker.) The initial parameters are selected as zero. We see that the desired isolation effect of the skyhook target is reached very quickly.

To examine the effect of the matrix P , we reduce P by a factor of 10, from $\text{diag}([1e14, 1e10, 3e8, 1e3])$ to $\text{diag}([1e13, 1e9, 3e7, 1e2])$. Figures 10 and 11 respectively show the time response and parameter estimates when the adaptive control turns on under 10 Hz base isolation. Comparing these two figures with Figures 4 and 8, we see that the transient time has become longer. The final values of the parameter adaptation are similar to those obtained before.

IV. CONCLUDING REMARKS

In this paper we experimentally study a new adaptive algorithm to achieve target dynamics (skyhook isolation) without model reference. This algorithm eliminates the necessity of base or ground vibration measurement and has the potential to improve transient performance. Its derivation is also based on Lyapunov analysis and Barbalat's lemma. The main idea here is to design a dynamic manifold for the target, rather than control the plant to follow the model

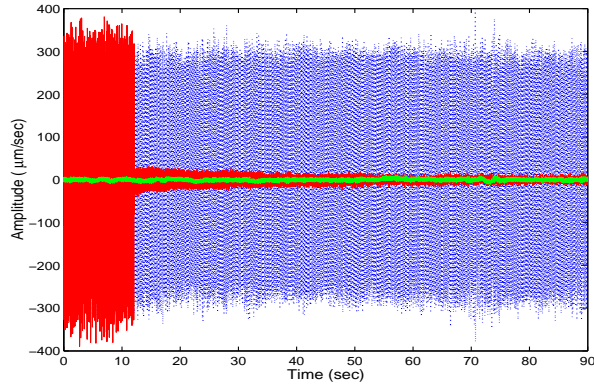


Fig. 10. Time response of isolated platform when adaptive control turns on, with a smaller P under 10 Hz base excitation with a smaller P . Base velocity (dot), platform velocity (solid), target skyhook velocity (dash)

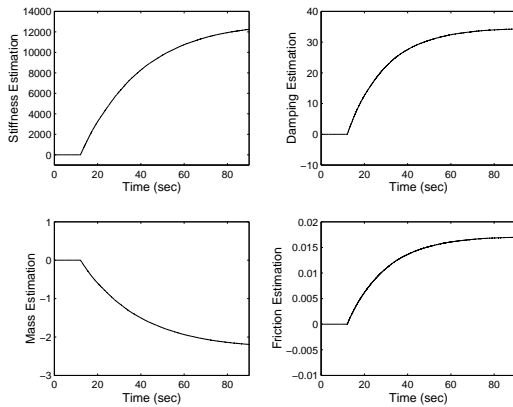


Fig. 11. Convergence of parameter estimations under 10 Hz base excitation with a smaller P : stiffness \hat{k} , damping \hat{c} , and mass \hat{m} , and friction \hat{f}

reference, so it can be taken as an extension of model-reaching sliding control [21], [22], [13] and adaptive sliding control [19].

The control and adaptation laws are derived for general single- or multi-DOF isolation systems, and the effects of geophone dynamics are also examined. We further carry out an experimental investigation based on a realistic plant with friction. The experiments indicate that this control strategy is highly effective for active vibration isolation without prior knowledge of system parameters. We also note that the choice of the matrices P and k_d is very important for the transient time. The strategy of performing real-time updates of the matrix P (see, [23]) might be used, or some slow updating schedule (to save computation) might be further explored.

In the foregoing we have assumed that the actuator placement matrix B is known; this requires us to have knowledge of the locations of the actuators and sensors. Although this is often the case, it might be more practical if we could extend the proposed adaptive control to include online estimation of the actuator-placement matrix B .

ACKNOWLEDGMENTS

The authors wish to thank MIT/Caltech LIGO Project, Prof. David Trumper and Dr. Osamah El Rifai of MIT

for kindly providing some hardware of the experiment. This research is partially supported by NSF Cooperative Agreement PHY-0107417.

REFERENCES

- [1] D. Karnopp, "Active and semi-active vibration isolation," *ASME Journal of Mechanical Design*, vol. 117, pp. 177–185, 1995.
- [2] D. Hrovat, "Survey of advanced suspension developments and related optimal control applications," *Automatica*, vol. 33, no. 10, pp. 1781–1817, 1997.
- [3] M. Serrand and S. Elliott, "Multichannel feedback control for the isolation of base-excited vibration," *Journal of Sound and Vibration*, vol. 234, no. 4, pp. 681–704, 2000.
- [4] D. Trumper and T. Sato, "A vibration isolation platform," *Mechantronics*, vol. 12, pp. 281–294, 2002.
- [5] A. G. Ulsoy, D. Hrovat, and T. Tseng, "Stability robustness of LQ and LQG active suspensions," *Journal of Dynamics Systems, Measurement, and Control*, vol. 116, pp. 123–131, 1994.
- [6] L. Zuo and S. Nayfeh, "Structured H2 optimization of vehicle suspensions based on multi-wheel models," *Vehicle System Dynamics*, vol. 40, no. 5, pp. 351–371, 2003.
- [7] M. R. Bai and W. Liu, "Control design of active vibration isolation using μ -synthesis," *Journal of Sound and Vibration*, vol. 257, no. 1, pp. 157–175, 2002.
- [8] J. Yang, Y. Suematsu, and Z. Kang, "Two-degree-of-freedom controller to reduce the vibration of vehicle engine-body system," *IEEE Transactions on Control System Technology*, vol. 9, no. 2, pp. 295–304, 2001.
- [9] S. Sommerfeldt and J. Tichy, "Adaptive control of two-stage vibration isolation mount," *Journal of Acoustical Society of America*, vol. 88, no. 3, pp. 938–944, 1990.
- [10] D. Karnopp, M. J. Crosby, and R. A. Harwood, "Vibration control using the semi-active force generators," *ASME Journal of Engineering for Industry*, vol. 96, pp. 619–626, 1974.
- [11] C. Kim and P. I. Ro, "A sliding mode controller for vehicle active suspension systems with nonlinearities," *Proc Instn Mech Engrs Part D, Journal of Automobile Engineering*, vol. 212, pp. 79–92, 1998.
- [12] M. Yokoyama, J. Hedrick, and S. Toyama, "A model following sliding mode controller for semi-active suspension systems with mr dampers," in *Proceedings of the American Control Conference*, 2001, 2652–2657.
- [13] L. Zuo and J. J. E. Slotine, "Robust vibration isolation via frequency-shaped sliding control and modal decomposition," submitted for publication.
- [14] Y. Sunwoo, K. Ceok, and N. Huang, "Model reference adaptive control for vehicle suspension systems," *IEEE Transactions on Control Systems Technology*, vol. 38, pp. 217–222, 1991.
- [15] A. Alleyne and J. K. Hedrick, "Nonlinear adaptive control of active suspensions," *IEEE Transactions on Control Systems Technology*, vol. 3, no. 1, pp. 84–101, 1995.
- [16] Y. P. Wang and A. Sinha, "Adaptive sliding mode control algorithm for multi-degree-of-freedom microgravity isolation system," in *Proceedings of the IEEE International Conference on Control Applications*, 1997.
- [17] F. Bakhtiari-Nejad and A. Karami-Mohammadi, "Active vibration control of vehicles with elastic body using model reference adaptive control," *Journal of vibration and control*, vol. 4, pp. 463–479, 1998.
- [18] Y. Zhang and A. Alleyne, "A new approach half-care active suspension control," in *Proceedings of the American Control Conference*, 2003, 3762–3767.
- [19] J. J. E. Slotine and W. Li, "On the adaptive control of robot manipulators," *International Journal of Robotics Research*, vol. 6, no. 3, pp. 49–59, 1987.
- [20] —, *Applied Nonlinear Control*. Prentice Hall, 1991.
- [21] B. Yao, S. Chan, and W. Gao, "Trajectory control of robot manipulator using variable structure model-reaching control strategy," in *International Conference on Control*, 1991.
- [22] K. D. Young and U. Ozguner, "Frequency shaping compensator design for sliding mode," *International Journal of Control*, vol. 57, no. 5, pp. 1005–1019, 1993.
- [23] G. Niemeyer and J. J. E. Slotine, "Performance in the adaptive manipulator control," *International Journal of Robotics Research*, vol. 10, no. 2, pp. 149–161, 1991.